

An Emissive C Analog Distinguishes  
between G, 8-oxoG, and T

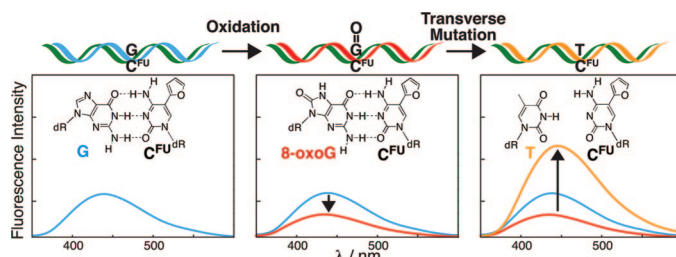
Nicholas J. Greco, Renatus W. Sinkeldam, and Yitzhak Tor\*

Department of Chemistry and Biochemistry, University of California,  
San Diego, 9500 Gilman Drive, La Jolla, California 92093-0358

ytor@ucsd.edu

Received November 25, 2008

## ABSTRACT



A minimally disruptive fluorescent dC analog provides a rapid and non-destructive method for in vitro detection of G, 8-oxoG, and T, the downstream transverse mutation product.

One of the most thoroughly examined DNA base modifications is 7,8-dihydro-8-oxoguanine (8-oxoG), a mutagenic product of oxidative damage by reactive oxygen species.<sup>1</sup> The presence of 8-oxoG is frequently viewed as a marker for cellular oxidative stress, a condition that has been linked to carcinogenesis.<sup>2</sup> The significance of this seemingly minor base damage results from 8-oxoG's ability to deceive DNA polymerases and form a stable (syn)8-oxoG•A base pair by presenting its Hoogsteen face, thereby mimicking T (Figure 1).<sup>3</sup> Unless repaired, this might cause G to T transversion mutations during DNA synthesis (Figure 1).<sup>4</sup> Not surprisingly, base-excision repair mechanisms have evolved to correct such deleterious base modification products.<sup>5</sup>

A non-destructive and real-time fluorescence-based detection of 8-oxoG, its repair, and induced mutation processes in oligonucleotides could significantly advance the in vitro bio-

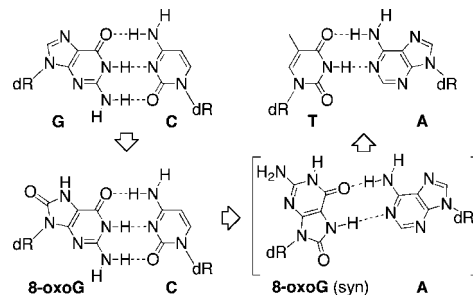


**Figure 1.** Base pairing along the DNA damage pathway from G•C to T•A (its transverse mutation product) via 8-oxoG.

chemical evaluation of this important DNA lesion.<sup>6</sup> It would complement existing procedures that rely on chromatographic, electrophoretic and immunological methods.<sup>7,8</sup> Toward this end, we hypothesized that one could take advantage of the distinct redox properties of 8-oxoG.<sup>9</sup> Electrochemical mea-

(1) (a) Beckman, K. B.; Ames, B. N. *J. Biol. Chem.* **1997**, *272*, 19633–19636. (b) Burrows, C. M.; Muller, J. *Chem. Rev.* **1998**, *98*, 1109–1152. (c) Bjelland, S.; Seeberg, E. M. *Mutat. Res.* **2003**, *531*, 37–80. (d) Cadet, J.; Douki, T.; Gasparutto, D.; Ravanat, J.-L. *Mutat. Res.* **2003**, *531*, 5–23. (e) Greenberg, M. M. *Biochem. Soc. Trans.* **2004**, *32*, 46–50. (f) Neeley, W. L.; Essigmann, J. M. *Chem. Res. Toxicol.* **2006**, *19*, 491–505. (g) Cooke, M. S.; Evans, M. D. *Proc. Natl. Acad. Sci. U.S.A.* **2007**, *104*, 13535–13536.

(2) (a) Ames, B. N.; Shigenaga, M. K.; Hagen, T. M. *Proc. Natl. Acad. Sci. U.S.A.* **1993**, *90*, 7915–7922. (b) Loft, S.; Poulsen, H. E. *J. Mol. Med.* **1996**, *74*, 297–312. (c) Wiseman, H.; Halliwell, B. *Biochem. J.* **1996**, *313*, 17–29. (d) Klaunig, J. E.; Kamendulis, L. M. *Annu. Rev. Pharmacol. Toxicol.* **2004**, *44*, 239–267. (e) Hirano, T. *J. Radiat. Res.* **2008**, *49*, 329–340.

(3) Leonard, G. A.; Guy, A.; Brown, T.; Teoule, R.; Hunter, W. N. *Biochemistry* **1992**, *31*, 8415–8420.

(4) Wood, M. L.; Dizdaroğlu, M.; Gajewski, E.; Essigmann, J. M. *Biochemistry* **1990**, *29*, 7024–7032.

(5) For recent reviews, see: (a) Fromme, J. C.; Verdine, G. L. *Adv. Protein Chem.* **2004**, *69*, 1–41. (b) David, S. S.; O'Shea, V. L.; Kundu, S. *Nature* **2007**, *447*, 941–950.

(6) 8-oxoG's low cellular abundance, complex localization, and chemical degradation pathways make the development of small probes for its intracellular detection a formidable task.

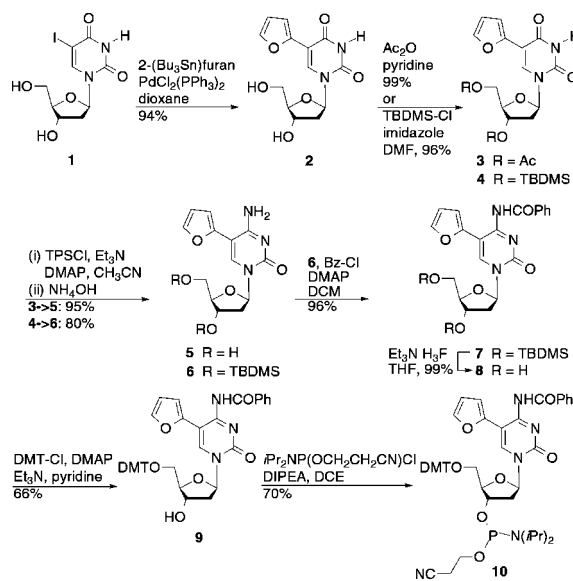
measurements show that 8-oxoG is more easily oxidized compared to G ( $E_{1/2} \approx 0.75$  and 1.3 vs NHE, respectively).<sup>9a,10</sup> Consequently, chemical approaches relying on 8-oxoG's susceptibility to oxidation and covalent trapping of the oxidized products in duplex DNA have been reported.<sup>11</sup> Since fluorescence quenching frequently occurs via photoinduced electron transfer (PET) mechanisms,<sup>12</sup> we suspected that 8-oxoG is likely to be a more effective quencher of certain fluorophores compared to G, its precursor.<sup>13</sup> Here we describe the design, synthesis, photophysical evaluation, incorporation, and implementation of a simple isomorphous fluorescent dC analog **5** that, upon incorporation into an oligonucleotide, photophysically distinguishes between 8-oxoG and G on the complementary strand. Not only is the damaged 8-oxoG-containing duplex highly quenched and the "repaired" G-containing duplex more emissive, the transverse mutated duplex containing T instead of G displays the most intense emission. This furan-containing emissive nucleobase therefore provides signature emission profiles for all key nucleobases involved in this DNA damage pathway (Figure 1).<sup>14</sup>

The primary design principle for minimally perturbing emissive nucleobases dictates maintaining the highest possible structural similarity to the natural nucleobases, while significantly improving their photophysical properties.<sup>15,16</sup> Specifically, an isolated absorption band for selective excitation, enhanced quantum yield over the native nucleobases, and sensitivity to changes in the microenvironment are desired.

Useful uridine-based nucleosides, fulfilling these criteria, were obtained by conjugating five-membered aromatic heterocycles such as furan at the 5 position (e.g., **2**).<sup>15–18</sup> Among the various heterocycles conjugated to dU, the furan moiety was found to yield the most favorable photophysical characteristics.<sup>15,17a</sup> We therefore anticipated the analogous furan-modified cytosine nucleobase to be emissive and responsive.

The 5-modified nucleosides are easily obtained using a coupling reaction between the 5-iodo substituted dU (**1**) and the corresponding stannylated heterocycles (Scheme 1). Con-

**Scheme 1.** Synthesis of Furan dC Analog **5** and Its Corresponding Amidite



(7) (a) Shigenaga, M. K.; Ames, B. A. *Free Radical Biol. Med.* **1991**, *10*, 211–216. (b) Muller, J. G.; Duarte, V.; Hickerson, R. P.; Burrows, C. J. *Nucleic Acids Res.* **1998**, *26*, 2247–2249. (c) Ropp, P. A.; Thorp, H. H. *Chem. Biol.* **1999**, *6*, 599–605. (d) Pouget, J.-P.; Douki, T.; Richard, M.-J.; Cadet, J. *Chem. Res. Toxicol.* **2000**, *13*, 541–549. (e) Soultanakis, R. P.; Melamede, R. J.; Bessalov, I. A.; Wallace, S. S.; Beckman, K. B.; Ames, B. N.; Taatjes, D. J.; Janssen-Heininger, Y. M. *Free Radical Biol. Med.* **2000**, *28*, 987–998. (f) Persinger, R. L.; Melamede, R.; Bessalov, I.; Wallace, S.; Taatjes, D. J.; Janssen-Heininger, Y. *Exp. Gerontol.* **2001**, *36*, 1483–1494. (g) Gore, M. R.; Szalai, V. A.; Ropp, P. A.; Yang, I. V.; Silverman, J. S.; Thorp, H. H. *Anal. Chem.* **2003**, *75*, 6586–6592.

(8) For fluorescence-based kinetic analysis of 8-oxoG DNA glycosylase; see: Kuznetsov, N. A.; Koval, V. V.; Nevinsky, G. A.; Douglas, K. T.; Zharkov, D. O.; Fedorova, O. S. *J. Biol. Chem.* **2007**, *282*, 1029–1038.

(9) (a) Oliveira Brett, A. M.; Piedade, J. A. P.; Serrano, S. H. P. *Electroanalysis* **2000**, *12*, 969–973. (b) Diclescu, V. C.; Chiorcea Paquim, A.-M.; Oliveira Brett, A.-M. *Sensors* **2005**, *5*, 377–393.

(10) (a) Berger, M.; Anselmino, C.; Mouret, J.-F.; Cadet, J. *J. Liq. Chromatogr.* **1990**, *13*, 929–940. (b) Goyal, R. N.; Dryhurst, G. *J. Electroanal. Chem.* **1992**, *135*, 75–91. (c) Yanagawa, H.; Ogawa, Y.; Ueno, M. *J. Biol. Chem.* **1992**, *267*, 13320–13326.

(11) (a) Xue, L.; Greenberg, M. M. *J. Am. Chem. Soc.* **2007**, *129*, 7010–7011. (b) Xue, L.; Greenberg, M. M. *Angew. Chem., Int. Ed.* **2007**, *46*, 561–564.

(12) Torimura, M.; Kurata, S.; Yamada, K.; Yokomaku, T.; Kamagata, Y.; Kanagawa, T.; Kurane, R. *Anal. Sci.* **2001**, *17*, 155–160.

(13) A modified G-clamp was reported to be quenched by 8-oxoG, but detecting the damaged base was limited to nucleosides in chloroform and micellar solutions. See: Nakagawa, O.; Ono, S.; Li, Z.; Tsujimoto, A.; Sasaki, S. *Angew. Chem., Int. Ed.* **2007**, *46*, 4500–4503.

(14) For other emissive C analogs, see: (a) Godde, F.; Toulme, J. J.; Moreau, S. *Nucleic Acids Res.* **2000**, *28*, 2977–2985. (b) Wilhelmsson, L. M.; Holmén, A.; Lincoln, P.; Nielsen, P. E.; Nordén, B. *J. Am. Chem. Soc.* **2001**, *123*, 2434–2435. (c) Liu, C. H.; Martin, C. T. *J. Biol. Chem.* **2002**, *277*, 2725–2731. (d) Okamoto, A.; Tainaka, K.; Saito, I. *J. Am. Chem. Soc.* **2003**, *125*, 4972–4973. (e) Berry, D. A.; Jung, K. Y.; Wise, D. S.; Serce, A. D.; Pearson, W. H.; Mackie, H.; Randolph, J. B.; Somers, R. L. *Tetrahedron Lett.* **2004**, *45*, 2457–2461. (f) Engman, K. C.; Sandin, P.; Osborne, S.; Brown, T.; Biller, M.; Lincoln, P.; Nordén, B.; Albinsson, B.; Wilhelmsson, L. M. *Nucleic Acids Res.* **2004**, *32*, 5087–5095. (g) Tinsley, R. A.; Walter, N. G. *RNA* **2006**, *12*, 522–529. (h) Marti, A. A.; Jockusch, S.; Li, Z. M.; Ju, J. Y.; Turro, N. J. *Nucleic Acids Res.* **2006**, *34*, e50. (i) Wojciechowski, F.; Hudson, R. H. E. *J. Am. Chem. Soc.* **2008**, *130*, 12574–12575.

version of the acetate-protected furan-modified dU analog **3** to the desired dC analog **5** is accomplished by activation of the 4 position as an aryl sulfonate ester followed by a displacement reaction with ammonia,<sup>19</sup> providing the fully deprotected furan-modified dC analog **5** (Scheme 1).<sup>17a,20</sup> Silyl protection of the furan-modified dU **4** facilitated the conversion to the dC analog **6** with retention of hydroxyl protection, thus allowing for standard benzamide protection of the exocyclic amine to give **7**. Desilylation and protection of the 5'-hydroxyl as the 4,4'-dimethoxytrityl derivative (**9**) followed by phosphorylation of the unprotected 3'-hydroxyl afforded **10**, the building block necessary for automated DNA synthesis (Scheme 1).<sup>20</sup>

The absorption spectrum of an aqueous solution of **5** shows, in addition to the typical high energy band seen in the parent

(15) Greco, N. J.; Tor, Y. *J. Am. Chem. Soc.* **2005**, *127*, 10784–10785. Greco, N. J.; Tor, Y. *Nat. Protoc.* **2007**, *2*, 305–316.

(16) Srivatsan, S. G.; Greco, N. J.; Tor, Y. *Angew. Chem., Int. Ed.* **2008**, *47*, 6661–6665.

(17) (a) Greco, N. J.; Tor, Y. *Tetrahedron* **2007**, *63*, 3515–3527. (b) Tor, Y.; Del Valle, S.; Jaramillo, D.; Srivatsan, S. G.; Rios, A.; Weizman, H. *Tetrahedron* **2007**, *63*, 3608–3614.

(18) (a) Srivatsan, S. G.; Tor, Y. *J. Am. Chem. Soc.* **2007**, *129*, 2044–2053. Srivatsan, S. G.; Tor, Y. *Tetrahedron* **2007**, *63*, 3601–3607. (b) Srivatsan, S. G.; Tor, Y. *Nat. Protoc.* **2007**, *2*, 1547–1555.

(19) Li, S.-N.; Piccirilli, J. A. *J. Org. Chem.* **2004**, *69*, 4751–4759.

(20) See Supporting Information for experimental details.

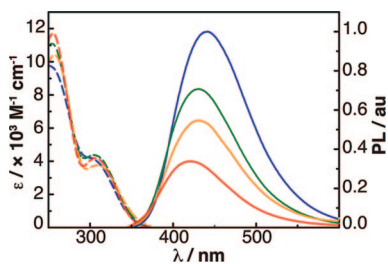


**Figure 2.** Absorption (dashed) and emission (solid) spectra of **5** in water (blue), methanol (green), dichloromethane (orange), and dioxane (red) at  $2.4 \times 10^{-5}$  M.

nucleoside, a clear shoulder at  $\sim 310$  nm (Figure 2). Excitation at this wavelength yields an emission profile with a maximum at 443 nm, which tails deeply into the visible range, with a relative quantum yield of 0.02 (Table 1).<sup>20,21</sup> Lowering solvent

**Table 1.** Photophysical Properties of Nucleoside **5** in Various Solvents<sup>20</sup>

| solvent         | $\lambda_{\text{abs}}$ (nm) | $\lambda_{\text{em}}$ (nm) | $\Phi$ | $I$ normalized |
|-----------------|-----------------------------|----------------------------|--------|----------------|
| water           | 310                         | 443                        | 0.020  | 1.00           |
| methanol        | 305                         | 439                        | 0.011  | 0.70           |
| dichloromethane | 309                         | 439                        | 0.009  | 0.54           |
| dioxane         | 309                         | 421                        | 0.006  | 0.33           |

polarity results in a better defined long wavelength absorption band ( $\lambda_{\text{max}} = 309$  nm) and a hypsochromic shift in emission maxima ( $\lambda_{\text{em}} = 421$  nm), which is associated with a hypochromic effect ( $I_{\text{Water/Dioxane}} = 3$ ) (Figure 2, Table 1).

Emission spectra of **5** in dioxane–water mixtures provide a more detailed view of the hypsochromic shift that arises upon decreasing the polarity of the chromophore’s microenvironment (Figure S2.1, Supporting Information).<sup>20</sup> Plotting the corrected emission energy maximum of **5** versus the microenvironment polarity described by  $E_{\text{T}}(30)$  values<sup>22</sup> results in a linear correlation (Figure 3).<sup>23</sup> Stern–Volmer titrations were conducted to determine the differences between G and 8-oxoG’s quenching abilities (Figure 4). Rewardingly, whereas G mini-

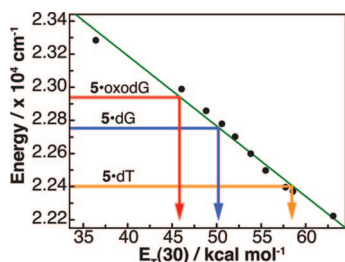


**Figure 3.** Correlating emission wavelengths with microscopic polarity  $E_{\text{T}}(30)$ <sup>22</sup> for nucleoside **5** (filled circles and green line)<sup>20</sup> and interpolation of corrected emission maxima<sup>23</sup> of duplexes containing **5** (arrows).

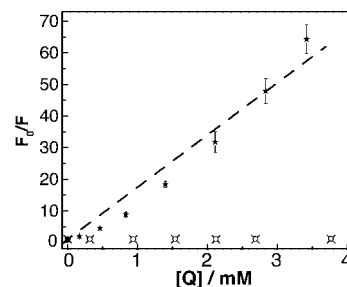


**Figure 4.** Steady-state Stern–Volmer plot for the titration of **5** with 8-oxo-2'-deoxyguanosine (stars, black dashed line), dGMP (X), and TMP (open circles). Some data and error bars were omitted for clarity (Figure S3.1 and Table S3.1, Supporting Information).<sup>20</sup>

mally impacted the emission of **5** ( $K_{\text{sv}} = 0.004 \text{ mM}^{-1}$ ), 8-oxoG was found to be a very effective quencher, even at low concentrations ( $K_{\text{sv}} = 16.5 \text{ mM}^{-1}$ ).<sup>20</sup>

To investigate the potential of the emissive nucleoside to photophysically discriminate between G, 8-oxoG, and T, an oligonucleotide that contains **5** at a central position was synthesized using **10** and standard solid-phase synthesis protocols (Figure 5).<sup>20</sup> All modified oligonucleotides were char-

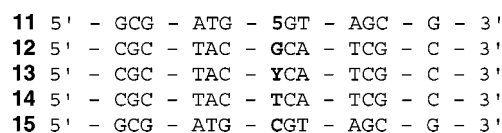


**Figure 5.** Oligonucleotide sequences where Y = 8-oxoG.

acterized using MALDI TOF MS.<sup>20</sup> Since modified C residues can, in principle, deaminate to yield the corresponding U derivatives, we unequivocally verified the presence of **5** and absence of **2** in the modified oligonucleotide **11**. Enzymatic digestion reactions, followed by HPLC analysis against all authentic nucleosides verified the presence of intact **5** and absence of **2** in the modified oligonucleotide **11** (Figure S6.1 and Table S6.1, Supporting Information).<sup>20</sup>

Oligonucleotide **11**, containing the furan-functionalized dC **5** was hybridized to three complementary oligonucleotides that contain either G (oligo **12**), 8-oxoG (oligo **13**), or T (oligo **14**) opposite the emissive nucleotide (Figure 5). Thermal denaturation (Table 2) and CD studies show no appreciable difference between the modified (**11**·**12**, **11**·**13**, and **11**·**14**) and unmodified duplexes (**15**·**12**, **15**·**13**, and **15**·**14**, respectively), suggesting the small furan modification does not disrupt duplex formation, stability, or structure (Figures S8.1 and S9.1, Supporting Information).<sup>20</sup>

The emission spectra of the furan dC containing duplexes, in both low (100 mM) and elevated (500 mM) ionic strength,

(21) Note that, although relatively low, this is easily detected by standard benchtop fluorimeters with excellent signal-to-noise.

(22) Reichardt, C. *Chem. Rev.* **1994**, *94*, 2319–2358.

(23) Fluorescence spectra were corrected according to  $I(\nu) = \lambda^2 I(\lambda)$ . See Lakowicz, J. R. *Principles of Fluorescence Spectroscopy*, 2nd ed.; Kluwer Academic/Plenum: New York, 1999.

**Table 2.** Thermal Denaturation of Control and Modified Oligonucleotides

| Duplex <sup>a</sup> | $T_m$ ( $\Delta T_m$ ) <sup>b</sup> | $T_m$ ( $\Delta T_m$ ) <sup>b</sup> |
|---------------------|-------------------------------------|-------------------------------------|
|                     | (°C) 100 mM NaCl                    | (°C) 500 mM NaCl                    |
| <b>15•12</b>        | 51.8                                | 59.2                                |
| <b>15•13</b>        | 47.7                                | 55.2                                |
| <b>15•14</b>        | 34.5                                | 41.2                                |
| <b>11•12</b>        | 51.5 (−0.3)                         | 59.0 (−0.2)                         |
| <b>11•13</b>        | 47.1 (−0.6)                         | 54.5 (−0.7)                         |
| <b>11•14</b>        | 34.7 (+0.2)                         | 42.0 (+0.8)                         |

<sup>a</sup>  $1.0 \times 10^{-6}$  M duplex DNA aqueous buffer pH = 7.0. <sup>b</sup>  $\Delta T_m$  = modified – unmodified.

are shown in Figure 6.<sup>23</sup> While the perfect duplex **11•12**, where G is placed opposite **5**, is significantly emissive, placing **5** opposite 8-oxoG (**11•13**) leads to considerable emission quench-

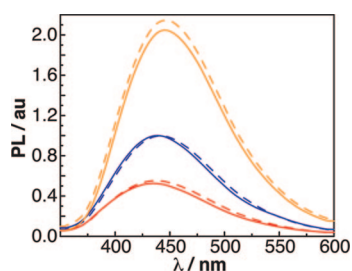


**Figure 6.** Steady-state emission spectra of oligonucleotides **11•12** (**5•G**, blue), **11•13** (**5•8-oxoG**, red), and **11•14** (**5•T**, orange) at  $5.0 \times 10^{-6}$  M in  $1.0 \times 10^{-2}$  M phosphate aqueous buffer pH = 7.0 containing  $1.0 \times 10^{-1}$  M NaCl (solid) and at  $4.6 \times 10^{-6}$  M in  $1.0 \times 10^{-2}$  M phosphate aqueous buffer pH = 7.0 containing  $5.0 \times 10^{-1}$  M NaCl (dashed).<sup>20</sup>

ing (ca. 2-fold), as hypothesized. Nucleoside **5** therefore clearly distinguishes between G and 8-oxoG, its oxidized product. In contrast, for duplex **11•14**, where **5** is placed opposite T, a substantial emission enhancement (ca. 4-fold compared to **11•13**) is observed (Figure 6, Table 3). Nucleoside **5** thus reports the presence of T, the ultimate transversion mutation product resulting from G oxidation to 8-oxoG, via enhanced emission. These observations, illustrating signature emission profiles for duplexes containing G, 8-oxoG, and T, suggest that the furan-modified dC nucleoside **5** could be utilized to follow, in vitro, DNA damage and its repair via this pathway using such emissive oligonucleotides.

The observed fluorescence quenching of **5** by 8-oxoG can be understood by the lower redox potential of 8-oxoG and concomitant higher potency as an excited-state quencher compared to G (Figure 4). Several observations collectively suggest that the substantial fluorescence enhancement observed for the **5•T** mismatch in **11•14** is due to exposure of the emissive nucleoside to a more polar environment, likely extrahelical.

Thermal denaturation data illustrates that the dC/T containing duplex **15•14** (as well as the analogous modified duplex **11•14**) are the least stable (Table 2). This is consistent with previous observations illustrating this particular dual pyrimidine mismatch to be rather unfavorable,<sup>24</sup> therefore suggesting a local structural perturbation. Fluorescence experiments carried out at elevated ionic strengths (500 mM) for all duplexes resulted in similar observations (Figure 6), rendering the potential higher abundance of the more emissive single strand due to poor hybridization unlikely.<sup>20</sup>

Further support for the proposed extrahelical residency of the fluorescent nucleobase is obtained by interpolating the emission energy of modified duplexes containing **5** and environmental polarity using the linear correlation shown above (Figure 3, Table 3). The emission spectra of the furanyl modified

**Table 3.** Emission Maxima of Modified Duplexes in Phosphate Buffers at Different NaCl Concentrations

| duplex       | $\lambda_{em}/nm$ ( $cm^{-1}$ ) | intensity at      | $\lambda_{em}/nm$ ( $cm^{-1}$ ) | intensity at      |
|--------------|---------------------------------|-------------------|---------------------------------|-------------------|
|              | 100 mM NaCl                     | $\lambda_{em}/au$ | 500 mM NaCl                     | $\lambda_{em}/au$ |
| <b>11•12</b> | 439 (22,779)                    | 1.00              | 440 (22,727)                    | 1.00              |
| <b>11•13</b> | 435 (22,989)                    | 0.52              | 437 (22,883)                    | 0.55              |
| <b>11•14</b> | 446 (22,422)                    | 2.05              | 447 (22,371)                    | 2.15              |

duplexes **11•12** and **11•13**, where furanyl dC **5** can pair in a Watson–Crick fashion, display emission maximum that correlate to relatively apolar environments (Figures 3 and 6, Table 3), while duplex **11•14**, where furanyl dC **5** is unable to pair in a W–C fashion with T, shows a red-shifted emission maximum that correlates to a polar environment, in agreement with an extrahelical disposition.

In summary, we have shown that an isomorphous fluorescent nucleoside **5** is a valuable probe for the detection of G, 8-oxoG, and its transverse mutation product T by eliciting markedly different emission intensities in conjunction with changes in emission maxima. The effective synthesis and incorporation of **5** could facilitate rapid and non-destructive real-time fluorescence-based methods for the in vitro monitoring of this DNA damage pathway.<sup>25</sup>

**Acknowledgment.** We thank the National Institutes of Health (GM069773) for support.

**Supporting Information Available:** Experimental procedures and biophysical data. This material is available free of charge via the Internet at <http://pubs.acs.org>.

OL802656N

(24) (a) Aboul-ela, F.; Koh, D.; Tinoco, I., Jr. *Nucleic Acids Res.* **1985**, *13*, 4811–4824. (b) Allawi, H. T.; SantaLucia, J., Jr. *Nucleic Acids Res.* **1998**, *26*, 2694–2701. (c) Hobza, P.; Sponer, J. *Chem. Rev.* **1999**, *99*, 3247–3276.

(25) To globally follow this pathway, an independent method, estimating the relative damaged/mutant population, might be needed.